Investigation of [^{18}F]2-Fluoro-2-Deoxyglucose for the Measure of Myocardial Glucose Metabolism

Michael E. Phelps, Edward J. Hoffman, Carl Selin, S. C. Huang, Gerald Robinson, Norman MacDonald, Heinrich Schelbert, and David E. Kuhl

University of California, Los Angeles, Los Angeles, California

F-18-labeled 2-deoxyglucose (FDG) was studied as a glucose analog for the measure of myocardial glucose metabolism. Myocardial uptake and retention, blood clearance, species dependence (dog, monkey, man), and effect of diet on uptake were investigated. Normal myocardial uptake of FDG was 3–4% of injected dose in dog and monkey, and 1–4% in man, compared with brain uptakes of 1.5–3% in dog, 5–6% in monkey, and 4–8% in man. The myocardial metabolic rate (MR) for glucose in the non-fasting (glycolytic) state was 2.8 times that in the fasting (ketogenic) state. Human subjects showed higher myocardial uptake after a normal meal than after-meal containing mostly free fatty aicds (FFA). Blood clearance was rapid with initial clearance $t_{1/2}$ of 0.2–0.3 min, followed by a $t_{1/2}$ of 8.4 ± 1.2 min in dog and 11.6 ± 1.1 min in man. A small third component had half-times of 59 ± 10 min and 88 ± 4 min in dog and man, respectively. With the ECAT positron tomograph, high image-contrast ratios were found between heart and blood (dog 3.5/1, man 14/1), heart and lung (dog 9/1, man 20/1), and heart and liver (dog 15/1, man 10/1). FDG was found to be taken up rapidly by the myocardium without any significant tissue clearance over a 4-hr period. FDG exhibits excellent imaging properties. Average counting rates of 12K, 20K, and 40K c/min-mCi injected are obtained in human subjects with high, medium, and low resolutions of the ECAT tomograph. Determination of glucose and FFA MR in vivo with ECT provides a method for investigation and assessment of changing aerobic and anaerobic metabolic rates in ischemic heart disease in man.

J Nucl Med 19: 1311–1319, 1978

Emission computed tomography (ECT) can produce images that quantitatively reflect the true tissue concentration of administered radiopharmaceuticals, and this has stimulated a growing interest in the use of the technique for the in vivo measurement of physiologic functions and metabolic rates (*1–3*). Since ischemic heart disease is a serious health problem, it is a major focus of study for new methods of diagnostic evaluation and therapy.

Most experimental data on myocardial substrate metabolism has been derived from the isolated rat and rabbit heart and open-chest, in situ dog and pig heart models (*4–9*). Although the results of these

Received Jan. 4, 1978; revision accepted June 22, 1978.

For reprints contact: M. E. Phelps, Div. of Nuclear Medicine, School of Medicine, University of California, Los Angeles, Los Angeles, CA 90024.

investigations have sometimes varied according to the method of study, several general statements can be made. In the *normoxic* heart perfused with free fatty acids (FFA) and glucose, FFAs are the major source of substrate for oxidative respiration. The amount of FFA uptake depends directly on plasma FFA concentration and on the rate of oxidative respiration. As oxidative respiration is reduced, under conditions of ischemia or anoxia, FFA acid uptake and oxidation are also reduced.

The metabolism of glucose in the aerobic heart depends upon the plasma concentration of glucose (and insulin), availability of alternative substrates (especially FFA), mechanical work, and rate of oxidative respiration (*4–9*). Under anoxic conditions the rate of glucose metabolism appears to be primarily a flow-related phenomenon. If coronary flow is maintained in anoxemia, glycolysis is accelerated, however, in ischemia, the rate of glycolysis may increase or decrease. This difference is probably related to decreased wash-out of metabolic breakdown products such as lactate and H^+, which inhibit glycolysis (*4–7*). It appears that the degree of inhibition of glycolysis is therefore related to the severity of the decrease in flow.

In the isolated perfused heart (Langendorff preparation) preliminary studies showed that [^{11}C] glucose had a low extraction and a relatively rapid turnover (*10*) in the "normal" perfusion states of this model—i.e., high-flow states of about 400 cc/min per 100 g to provide normal oxygen delivery in the absence of hemoglobin. While these investigators carried out in vivo studies under normal and ischemic conditions in the dog with [^{11}C] palmitic and and [^{11}C] octanoic acid, no in vivo studies were done with [^{11}C] glucose (*10*).

Recently, Ido et al. have successfully used F-18 to label 2-deoxy-2-fluoro-D-glucose, FDG, (*11,12*). Studies in dogs, monkeys, and humans by Phelps et al. (*13*) and in rats and dogs by Gallagher et al. (*14*) have shown that FDG has a significant extraction by the myocardium with a slow clearance [$t_{1/2} >> 2$ hr, Gallagher et al. (*14*)]. The work of these investigators suggests that FDG could be used to study glucose metabolism in the heart.

In this work we have used the ECAT* positron imaging system (*1,2,13,15*) to investigate the myocardial uptake and retention of FDG, its blood clearance rates, the species dependence (dog, monkey, man) of myocardial uptake, and the effect of diet on myocardial uptake. Image contrast ratios between myocardium, blood, lung and liver, and system count rate per intravenous dose, have also been measured with the ECAT. These studies were carried out to examine whether FDG would be suitable for the noninvasive in vivo measure of myocardial metabolic rate for glucose with ECT.

MATERIALS AND METHODS

Preparation of FDG. FDG was prepared after the method developed by the chemistry group at Brookhaven National Laboratory (*11,12*). $^{18}F_2$ was produced using the $^{20}Ne(d,\alpha)^{18}F$ reaction with 11-MeV deuterons on a target containing 1.1% F_2 in neon. $^{18}F_2$ is subsequently swept (with He) into a reaction vessel containing 3,4,5-tri-0-acetyl-D-glucal to form [^{18}F]3,4,6-tri-0-acetyl-2-deoxy-2-fluoro-D-glucopyranosyl fluoride, which was purified by liquid chromatography (silica gel) by elution with a 4:1 mixture of petroleum ether and diethyl ether. Subsequent acid hydrolysis and removal of ($^{18}F^-$) with an alumina column gave FDG. The overall radiochemical yield is about 10% with a purity >95%.

Animal preparations. Ten dogs and three rhesus monkeys were lightly anesthetized with sodium pentobarbital (20 mg/Kg). A femoral arterial catheter was used for determination of glucose concentration and FDG blood clearance rate, and a femoral vein catheter for injection of FDG. These animals were used for either the determination of blood clearance rates and/or whole-body rectilinear scans and tomographic studies.

Blood clearance. FDG was injected intravenously over a 30-sec interval and arterial blood samples taken; starting at time zero, a sample was taken every 15 sec for 1 min, every minute for the next 5 min, and the interval was then progressively lengthened as samples were drawn for the next 1–4 hr. Blood samples, for measurement of FDG and plasma glucose concentration were immediately placed into an ice bath. FDG plasma data were corrected for radioactive decay, plotted, and analyzed to determine clearance rates. Plasma glucose levels were measured by standard colorimetric techniques in triplicate.

ECAT studies. All the animal and human imaging studies with the ECAT were carried out using i.v. injections of 0.5–5 mCi of FDG. All quantitative studies were preceded by transmission scans for correction of photon attenuation in the subject (*16*). The rectilinear emission scans were used to study the whole-body distribution of FDG, and the transmission scans to select levels to be studied in detail with ECT (see Fig. 5).

The myocardial accumulation rate for FDG was studied with ECT scans of a single cross section of the heart using the following sequence: images were made every 30 sec for the first 5 min after injection, 3 min images were then made for the next 9 min, and progressively longer imaging times were then

used to follow myocardial tissue activity for another 4 hr. In all other studies, 40–50 min after injection were allowed to establish a steady-state (or near-steady) condition before scanning. Regions of interest of the left ventricle were selected for the measurement of tissue activity as a function of time. The scan times for whole-body rectilinear scan studies varied from 10 to 40 min (three views), and 2–3 min for limited-field views of the thorax (three views). Scan times of 4–7 min/slice were used in the ECT studies, depending on the amount of FDG injected and time after injection.

The high (HR), medium (MR), and low (LR) resolutions of the ECAT in the tomographic mode are 0.95, 1.3, and 1.7 cm, respectively, in the cross-section plane, with a slice thickness of about 1.9 cm (*1,15*). In the rectilinear scan format they are 0.85, 1.3, and 1.8 cm, respectively (*15*). The tomograph was calibrated daily with a phantom 20 cm in diameter containing a known amount of positron activity, which allows the determination of the tissue activity concentration in units of μCi/cc.

Calculation of metabolic rate. The myocardial metabolic rate for a glucose (MR) could be calculated for EDG if the rate constants for transport, enzymatic phosphorylation, glucose-6-PO_4 utilization, and FDG distribution volumes were known (*17*). Although these values are known for brain, they have not yet been determined for the myocardium. Without them, however, one can still calculate a relative index of MR that allows MR ratios to be determined rather than the absolute values. Using an approximate form of the model developed by Sokoloff et al. (*17*) for the cerebral metabolic rate for glucose, all the constants can be lumped into a single term, K, and the metabolic rate is given by†

$$MR \cong \frac{K\,[Glu]\,C_T}{\int_0^T C_b(t)\,dt}, \qquad (1)$$

where [*Glu*] is the capillary plasma glucose concentration, C_T is the FDG-6-PO_4 tissue concentration at time T (mean time of ECT measurement), and $C_b(t)$ is the FDG capillary plasma concentration at any given time between injection and time T. Although the arterial [*Glu*] and $C_b(t)$ values were used in Eq. 1, the venous values across a resting arm or leg have been shown preliminarily to give a good approximation of capillary values (*18*). The tissue concentration, C_T, is measured from the tomographic image in μCi/g. The integral in the denominator of Eq. 1 is the area, A, under the blood curve from 0 to time T in units of (μCi/cc) $\times$ time, and [*Glu*] is in units of mg/cc. Thus, Eq. 1 can be reduced to

$$MR = \frac{K\,[Glu]\,C_T}{A}, \qquad (2)$$

where MR is in glucose utilization units of mg glucose/unit time, per gram of tissue.

In fasting studies carried out in this work, the metabolic rate for glucose was varied from one state (MR_1) to another (MR_2) to give

$$MR_1 = \frac{K\,[Glu]_1\,C_{t,1}}{A_1} \qquad (3)$$

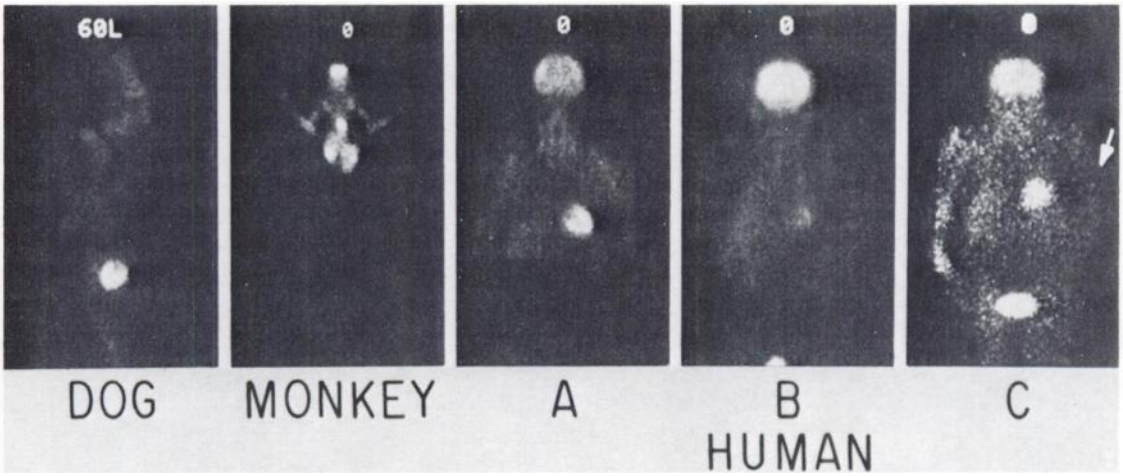

FIG. 1. Rectilinear scans with ECAT showing whole-body distribution of intravenously injected FDG in dog, monkey and man. Dog: 20-min scan performed 90 min after injeciton of four mCi of FDG. Study was performed about 2 hr after morning meal. Note high uptake in heart and low uptake in brain. Monkey: 20-min scan performed 30 min after injection of 1 mCi FDG. Scan was performed about 2 hr after morning meal. Note high uptake in both brain and heart. Human (A): 20-min rectilinear scan performed 2 hr after injection of 8 mCi of FDG. Study was performed 2 hr after normal meal containing substantial amounts of sugar. Note high uptake in both brain and heart. Human (B): 40-min rectilinear scan 40 min after injection of 2 mCi FDG. Study was performed 1 hr after meal containing high level of free fatty acids. Note high uptake in brain and low uptake in heart. Human (C): 40-min rectilinear scan 90 min after injection of 0.4 mCi of FDG in patient with left-sided hemiparesis. Note high uptake in brain and heart and low uptake in paralyzed arm (arrow).

and

$$MR_2 = \frac{K\,[Glu]_2\,C_{t,2}}{A_2}. \qquad (4)$$

In taking the ratio between Eqs. 3 and 4 (MR_1/MR_2) the undetermined value of K cancels.

Glycolytic/ketogenic MR. To measure the effect of fasting and nonfasting states, a 20-kg dog was fasted for 2½ days, anesthetized, and catheters placed in the femoral artery and a saphenous vein. FDG (0.7 mCi) was injected i.v. and blood samples withdrawn for measurement of plasma glucose and the FDG blood curve. Six tomographic slices of the thorax, separated by 15 mm, were taken with images starting 40–50 min after injection.

One hour later the dog was infused i.v. with 10% glucose and 25 units of insulin for 20 min, followed by an injection of 2.5 mCi of FDG; the scanning procedure was then repeated with continuous glucose infusion (400 cc total). The residual F-18 activity from the previous scan was measured by performing scans as a function of time until the second injection, and extrapolating these data to the times of the subsequent scans. (This resulted in a correction of about 18%.) For control, a similar study of the same dog was run a month later without the fasting.

RESULTS

Whole-body distribution. Figure 1 shows the whole-body distributions of FDG, following i.v. injection, in dog, rhesus monkey, and man and illustrates the differences due to species and diet. The dog and monkey studies were performed about 3 hr after their morning meal. Whereas the dog typically shows a higher uptake in the heart [3.4 ± 1.1 (mean ± s.d.) % of injected dose], compared with the brain (1.8 ± 0.4), the monkey shows similar or lower uptake in heart (3.7 ± 0.8) compared with brain (5.9 ± 0.6).

The three images of man (Fig. 1) illustrate distributions in a volunteer (A) 3 hr after a normal breakfast; (B) a normal human volunteer studied after eating a meal containing mainly free fatty acids; and (C) a patient with left-sided hemiparesis. In this work the normal cerebral uptake of FDG in man was found to be about 4–8% (6.3 ± 1.8) of the injected dose. The myocardial uptake in man varied from about 1 to 4% (3.3 ± 1.0).

Glycolytic/ketogenic metabolic ratio. The index of myocardial metabolic rate for glucose (MR_1) was calculated for six cross-sectional levels of the left ventricle (Fig. 2) for the dog that was fasted 2.5 days. The arterial plasma glucose values during the experiment were relatively constant (78.5 ± 2.0 mg%; mean ± s.d.). Following glucose plus insulin infusion, the arterial plasma glucose values were higher and somewhat more variable (112 ± 15 mg%). The calculated index of the metabolic rate for glucose in this state (MR_2) was dramatically in-

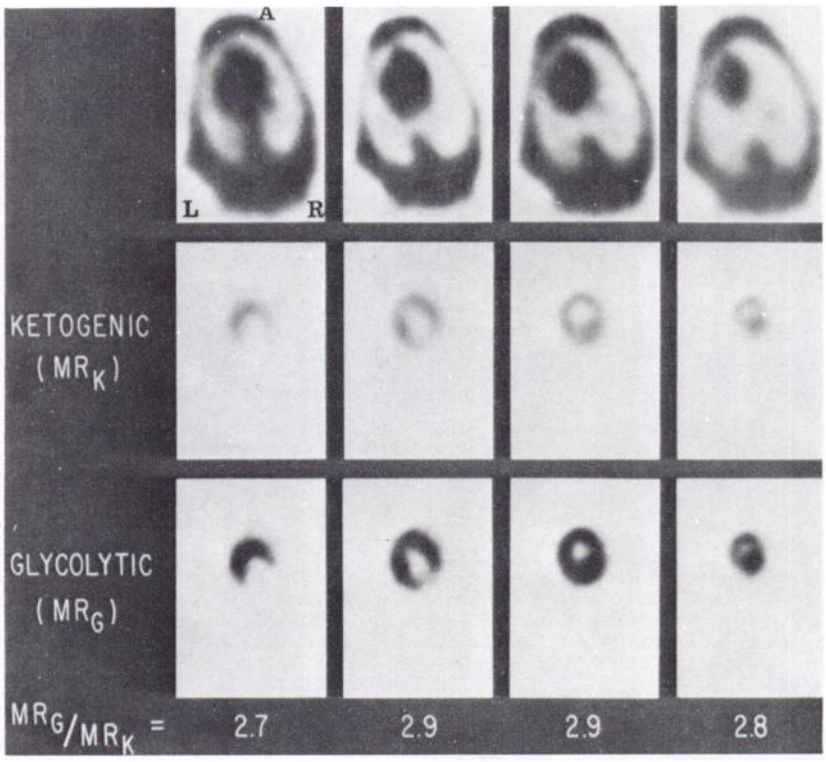

FIG. 2. Tomographic study of dog's myocardial glucose metabolism in ketogenic state from 2½ days of fasting, and in glycolytic state from infusion of glucose and insulin. Top: reconstructed transmission images of thorax from levels at base to apex of heart. Middle: cross-sectional tomographic images showing glucose metabolic rate in left ventricle during ketogenic state. Bottom: same cross-sectional levels as shown above, taken after second injection of FDG subsequent to 20-min infusion of glucose that was continued throughout study to bring animal into glycolytic state of metabolism. Numerical values shown at bottom are slice-by-slice ratios for glycolytic metabolic rate over ketogenic MR. Resolution was medium and images were ungated.

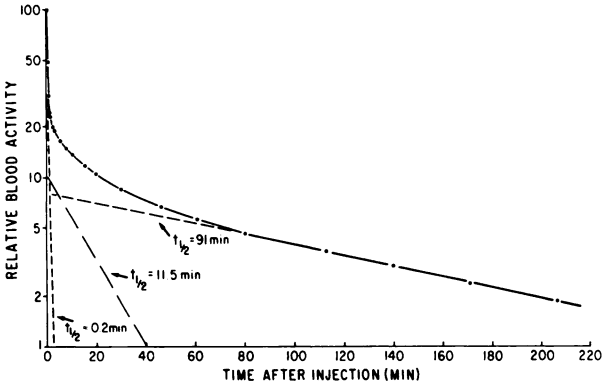

FIG. 3. Arterial blood curve subsequent to i.v. injection of FDG. Solid dots indicate measured values, and dashed lines indicate three exponential components that best fit measured data. These components should not be taken as compartments and are shown only to indicate the major features of the blood-clearance curves.

creased over the previous metabolic state ($MR_2/MR_1 = 2.8 \pm 0.1$; see Fig. 2).

The same sequence of measurements as above were repeated with the same dog but without fasting (control study). The arterial plasma glucose values in the first set of measurements of MR were constant during the course of the study (87.7 ± 2.1). The plasma glucose values were higher during the second part (i.e., during glucose infusion) but remained relatively constant (202 ± 10 mg%). The average ratio of MR_2/MR_1 from six cross sections of the left ventricle was found to be 0.96 ± 0.07.

The above results indicate that the MR index is sensitive to real metabolic changes, since the measured MR changed during physiologic alteration of fasting, whereas no change was observed during passive alteration of blood glucose.

Blood clearance of FDG. FDG was found to clear rapidly from the blood, as shown in Fig. 3. The arterial-blood clearance curves for six dogs and four human subjects can be approximated by three components. The major component had a half-time of about 0.2–0.3 min for both dog and human subjects. The second component had a half-time of 5–10 min (8.4 ± 1.2 min) in dogs and 10–13 min (11.6 ± 1.1 min) in man, whereas the third component had a half-time of 40–80 min (59 ± 10 min) in dogs and 80–95 min (88 ± 4 min) in man. The major portion of the fast component probably results from the dilution of the injected FDG in the total blood pool and extraction by highly perfused tissues before equilibration is established. The remaining clearance is due to continued metabolic extraction and also to clearance by the kidneys. These three components should not be taken as three compartments, since FDG is extracted by all the perfused tissue; the three components are somewhat artificial and are given only to indicate the characteristics of the blood-clearance.

TABLE 1. IMAGE-CONTRAST RATIOS IN FDG MYOCARDIAL STUDIES

	L.V./R.V.†	L.V./blood‡	L.V./lung	L.V./liver
Dog*	2/1	3–4/1	8–10/1	10–12/1
Human*	2.5/1	12–16/1	12–30/1	6–12/1

* Range of values at cross-sectional levels from base to near apex of heart. Three dogs contributed (12 levels total), and one human subject (six levels). Time after injection was 40–60 min in both dog and human.
† L.V. = left ventricle; R.V. = right ventricle.
‡ Blood in left-ventricular chamber.

Imaging characteristics of FDG. A selected series of cross-sectional images of the thorax in a dog and a human volunteer after the i.v. injection of FDG are shown in Figs. 4 and 5. These images show mainly the left ventricle, although the first levels in each study also show the right ventricle. The image contrast ratios of FDG in the left ventricle a) to the right ventricle, b) to the blood pool of left ventricle, c) to the liver, and d) to the lung are shown in Table 1. Examples of histogram profiles across selected levels for a human study are shown in Fig. 5. Considering that these studies were performed in the medium-resolution mode and were ungated, the image-contrast ratios of myocardium to blood, lung, and liver are very high.

In the normal human subject (e.g., Fig. 5), average counting rates of 40K, 20K, 12K c/min per mCi injected i.v. were measured for the low (1.7 cm), medium (1.3 cm), and high (0.95 cm) ECT resolution.

A fundamental assumption of Eq. 1 is that blood FDG activity level in the myocardial tissue is small compared with the intracellular FDG-6-PO_4. An estimate of this can be obtained from the image-contrast ratio of myocardium to blood in left-ventricular chamber of about 14:1 in humans at a time ≧40 min post injection (Table 1). Assuming a myocardial blood volume of 8%, an intertissue volume for free glucose of 15% (*19*), and a tissue-to-blood concentration ratio for glucose of about 0.9 (J. Bassingthwaighte, unpublished data), then more than 95% of the F-18 tissue activity is in the form of FDG-6-PO_4.

Myocardial tissue uptake. Initially, FDG is rapidly taken up by the myocardium and then continues to accumulate slowly from the FDG in the blood, as shown in Figure 6.

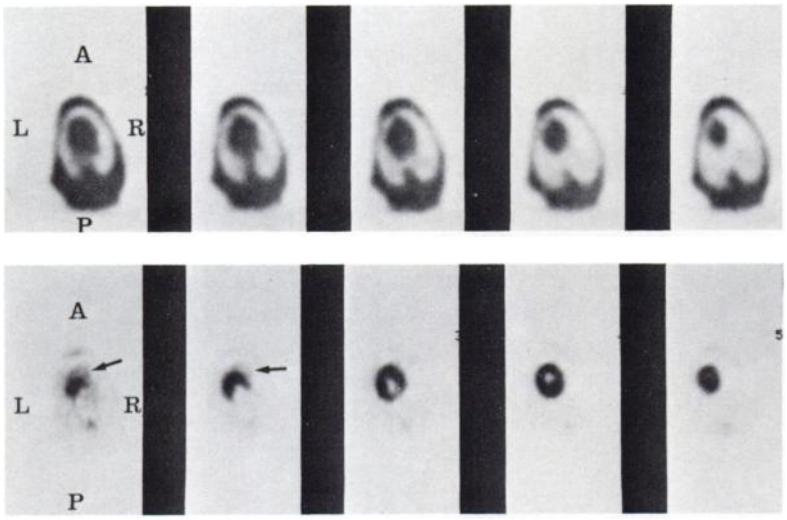

FIG. 4. Tomographic study (bottom row) of 20-kg dog started 40 min after i.v. injection of 0.4 mCi FDG. Scan time was 5 min per slice, each containing about 700,000 counts. Resolution was medium and study was ungated. Levels are from base to apex in 15-mm steps and major structure seen is left ventricle. Right ventricle (arrow) is seen in first level at left but is difficult to image because of its lower metabolic rate and size. Reconstructed transmission images are shown at top.

DISCUSSION

Our in vivo values for the percentage uptake of FDG in heart and brain in the dog and monkey are in relatively good agreement with the in vitro values of Gallagher et al. (*14*). The variation in the percentage uptake in the human brain was primarily dependent (in normal subjects) upon the level of blood glucose (i.e., the higher level of blood glucose, the lower the extraction fraction of glucose and FDG) and diet (at a substantial time after the meal the whole-body respiratory quotient drops and the rest of the body extracts a smaller amount of glucose and FDG). The large variations in myocardial uptake of FDG are due not only to variations in extraction from changing levels of blood glucose, but they also result because glucose is a secondary substrate to FFA under normal conditions of myocardial metabolism (*4–9*).

Our in vivo ratios for the uptake in the left ven-

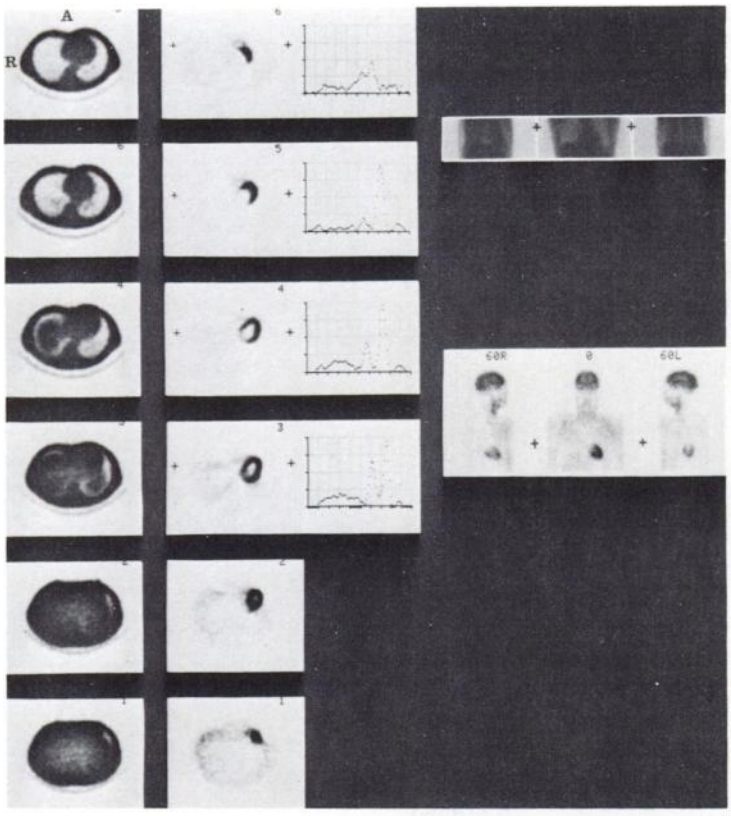

FIG. 5. Tomographic study of myocardial glucose metabolism in human volunteer. Left: reconstructed transmission images. Center: reconstructed emission images with histogram profiles through levels indicated by crosses on images. Scans are from level of base to apex of heart in 18-mm steps, performed 40 min after i.v. injection of 4.6 mCi of FDG. Resolution was medium, scan times were 7 min per slice, and images contain 400,000 to 600,000 counts per slice. Scans were ungated. Major structure seen is left ventricle. Right ventricle is seen in upper two images. Note ratio between right ventricle in top image and left ventricle in lower images; also ratio of left ventricle to blood pool in second and third images from top, and left ventricle to lung and liver in second, third, and fourth images from top. Right: Limited-field rectilinear scan in transmission mode (3-min scan) and emission mode (3-min scan) used for identification and setup for tomographic scans. Rectilinear scans have three views: A-P and two ±60° oblique views that are obtained simultaneously with ECAT. Scan levels are selected for tomography with a joy stick on console that indicates level by crosses on rectilinear image. Resolution was medium and scans were ungated.

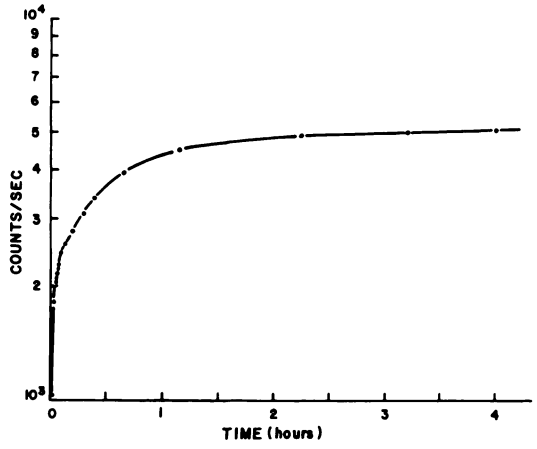

FIG. 6. Accumulation curve of DG in myocardial tissue as it is continually extracted from the blood and trapped in cells as DG-6-PO_4. Extraction rate is initially high due to high initial FDG blood concentration; it then slowly decreases as blood concentration falls with time (see blood curve in Fig. 3).

tricle over those in liver and lung (Table 1), obtained in dog and man, are considerably higher than the corresponding ratios for dog, and lower than those for rat, obtained from in vitro studies with FDG (*14*). The in vivo ratio of left to right ventricle was about 2.3/1, which is in good agreement with the average in vitro value of 2.1 in dogs with FDG (*14*).

The ratio of glycolytic to ketogenic myocardial metabolism (2.8 ± 0.1) found in this work is in excellent agreement with the 2.9 reported in the literature (*20*) for the ratio of the myocardial metabolic rate for carbohydrates between human fasting and nonfasting. Our fasting dog had been driven into a state of aerobic metabolism, deriving its metabolic energy almost exclusively from FFA. The infusion of glucose with insulin provided a source of glucose, allowing a more nearly normal balance of, and interrelationship between, myocardial substrates in or supplied to the blood. The nonfasted dog could be assumed to have adequate substrate levels during all scans. The fact that MR remains constant in the nonfasted dog even when the blood glucose is markedly elevated, results because in the normal well-oxygenated state, there is a maintained balance between myocardial metabolism of FFA and glucose in which there is a preference for metabolism of the high-energy content FFA (*4–9*). A variation in the utilization rates of these two substrates is not passively dependent upon the blood glucose level in the normoxic state when sufficient blood FFA and glucose are present.

Although we have not yet measured the kinetic rate constants for FDG in the myocardium, the uptake and long retention seen in these studies and the in vivo work of Gallagher et al. (*14*) are consistent with the hypothesis that in the myocardium FDG competes for transport sites and hexokinase in the same manner as has been determined in the brain from in vitro studies with [^{14}C] deoxyglucose (*17*) and FDG (*21*). The FDG-6-PO_4 appears to be formed and trapped in the myocardium as in the brain, due to its low cellular membrane permeability (Fig. 7) and the low activity of glucose-6-phosphatase (*4*) for conversion of FDG-6-PO_4 back to FDG, which can diffuse out of the tissue into the blood.

The low liver uptake seen in this work (at >40 min post injection) and the rapid clearance from the liver found by Gallagher et al. (*14*) suggest that FDG is not converted to glycogen (through glucose-1-phosphate) for storage in the liver (see Fig. 7). Sole and Crane (*22*) have shown that 2-deoxyglucose does inhibit the conversion of DG-6-PO_4 to DG-1-PO_4 for incorporation into glycogen (Fig. 7). In addition, the liver has a high concentration of glucose-6-phosphatase to convert glucose-6-PO_4 (FDG-6-PO_4) to glucose (FDG) (*23*), which then diffuses back into blood stream (liver acts as a blood-glucose buffer). This is consistent with our findings and that of Gallagher et al. (*14*) in that FDG is not retained by the liver; it also provides the explanation for the high image-contrast ratio between myocardium and liver.

The above discussion also implies that FDG is specific for myocardial glycolysis from glucose supplied by the circulating blood, rather than from the composite source of blood and intracellular glycogen. This could appear as a problem, since the glucose metabolic rate measured with FDG would not reflect that portion derived from glycogen. The amount of glycogen stored in myocardial cells is small (*20*), however, and can provide glucose only for a short time. Glycogen metabolism is a transient phenomenon that is initiated by cyclic AMP through the activation of phosphorylase 'a' (Fig. 7). In acute anoxia the energy requirements of the heart can be sustained by glycolysis from glycogen alone for only about 4.2 min (*20*).

FDG exhibits a number of important characteristics for the imaging of the myocardial metabolic rate for glucose in vivo with positron tomography. It has rapid tissue uptake, long-term retention in the tissue, and rapid blood clearance. Our blood clearance rates are also in good agreement with the data of Gallagher et al. (*14*). The rapid blood clearance is important for two reasons when ECT is used to image and measure the myocardial metabolic rate for glucose (MR). First, the physiologic compartmental model (approximate form given by Eq. 1)

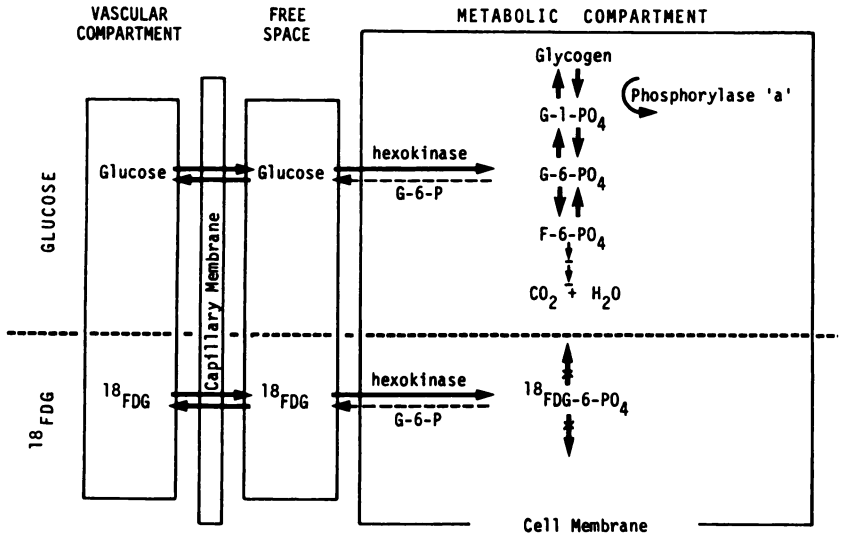

FIG. 7. Simplified schematic representation of myocardial utilization of glucose and a physiologic analog, 2-deoxyglucose labeled with F-18 (FDG). G-6-PO_4 is glucose-6-PO_4; G-1-PO_4 is glucose-1-PO_4; F-6-PO_4 is fructose-6-PO_4. FDG competes with glucose for transport sites in the capillary and cell membrane and for hexokinase, the enzyme for converting glucose to glucose-6-PO_4. FDG is trapped in myocardial cells as FDG-6-PO_4, since the enzymatic conversion to G-1-PO_4 and F-6-PO_4 is inhibited by the 2-deoxy analog of glucose and low membrane permeability to DG-6-PO_4. Slow tissue clearance of FDG-6-PO_4 shown in this work indicates that cellular concentration of glucose-6-phosphatase (G-6-P), which converts FDG-6-PO_4 back to FDG, must be low. Note that glycolysis can occur from both exogenous (cellular glycogen) sources, whereas FDG is specific to the exogenous route.

for the measure of MR assumes that FDG is rapidly cleared from the blood and accumulates in tissue such that at a reasonable time after injection (30–40 min) most of the activity in the organ is intracellular in the form of FDG-6-PO_4 (*17,21*). Second from an imaging point of view, the blood activity in the ventricular chambers should be low enough to minimize interference with the measurement of activity in the myocardial tissue. In combination with positron tomography, the FDG images provide high contrast between myocardium, blood, lung, and liver.

FDG appears to be an excellent tracer for the in vivo study of myocardial metabolic rate for exogenous glucose in normal, hyper-, and hypometabolic states. FDG and labeled FFA (e.g., [^{11}C] palmitic acid) in combination with positron tomography will allow characterization of regional anaerobic/aerobic myocardial metabolic rates and a measure of the working energy state of the myocardium.

The changes in FFA and glucose metabolism during the graded levels of ischemia that are present in different degrees of human ischemic heart disease are still poorly defined, and therefore this approach could improve our understanding of this disease entity.

FOOTNOTES

* ORTEC, Inc., Oak Ridge, TN.

† This approximate form assumes that sufficient time after injection has been allowed for FDG to be in or close to a true steady-state condition and that tissue FDG concentration is small. At 40–50 min after injection this is a good approximation (Phelps, unpublished work; see also Results section). A more exact model of MR can be applied after the kinetic constants of FDG in heart have been determined.

ACKNOWLEDGMENTS

We thank Joann Miller, Francine Aguilar, and Anthony Ricci, for technical help. Thanks are also due to Larry McConnel, Ross Birdsall, and Joseph Cook of the cyclotron group and to Mary Lee Griswold and Hector Pimentel for illustration work. We also acknowledge the helpful discussions with Drs. Louis Sokoloff and Charles Kennedy of Cerebral Metabolism Laboratory at the National Institutes of Health, and with Dr. Robert Marshall of the Division of Cardiology, UCLA.

This work was partially supported by ERDA Contract EY-76-C-03-0012 Gen-12, NIH grant 7R01-GM 24839-01.

REFERENCES

1. PHELPS ME: Emission computed tomography. *Sem Nucl Med* 7: 337–365, 1977

2. PHELPS ME, HOFFMAN EJ, KUHL DE: Physiologic Tomography: A new approach to measure of metabolism and physiologic function. In *Medical Radionuclide Imaging*, vol. 1, IAEA, Vienna, Austria, 1977, pp 233–253

3. TER-POGOSSIAN MM, PHELPS ME, BROWNELL GH, et al: *Reconstruction Tomography in Diagnostic Radiology and Nuclear Medicine.* Baltimore, University Park Press, 1977

4. NEELY JR, MORGAN HE: Relationship between carbohydrate and lipid metabolism and the energy balance of heart muscle. *Annual Rev Physiol* 36: 413–459, 1974

5. OPIE LH, OWEN P, RIEMERSMA RA: Relative rates of oxidation of glucose and free fatty acids by ischaemic and non-ischaemic myocardium after coronary artery ligation in the dog. *Europ J Clin Invest* 3: 419–435, 1973

6. ROVETTO MJ, LAMBERTON WF, NEELY JR: Mechanisms of glycolytic inhibition in ischemic rat hearts. *Circ Res* 37: 742–751, 1975

7. HILLIS LD, BRAUNWALD E: Myocardial ischemia. *N Engl J Med* 296: 971–978, 1034–1041, 1093–1096, 1977

8. WILDENTHAL K, MORGAN HR, OPIE LH, et al, eds: *Regulation of Cardiac Metabolism.* American Heart Association Monograph No. 49. Dallas, The American Heart Assoc., Inc., 1976

9. BRAUNWALD E, ed: *Protection of the Ischemic Myocardium.* American Heart Association Monograph No. 48. Dallas, The American Heart Assoc., Inc., 1976

10. WEISS ES, HOFFMAN EJ, PHELPS ME, et al: External detection and visualization of myocardial ischemia with

^{11}C-substrates in vitro and in vivo. *Circ Res* 39: 24–32, 1976

11. IDO T, WAN CN, CASELLA V, et al: Labeled 2-deoxy-D-glucose analogs. ^{18}F-labeled 2-deoxy-2-fluoro-D-glucose, 2-deoxy-2-fluoro-D-mannose and ^{14}C-2-deoxy-2-fluoro-D-glucose. *J Label Comp Radiopharm* 14: 175–183, 1978

12. IDO T, WAN CN, FOWLER JS, et al: Fluorination with F_2. A convenient synthesis of 2-deoxy-fluoro-D-glucose. *J Org Chem* 42: 2341–2342, 1977

13. PHELPS ME, HOFFMAN EJ, HIGHFILL R, et al: A new emission computed axial tomograph for positron emitters. *J Nucl Med* 18: 603, 1977 (abst)

14. GALLAGHER BM, ANSARI A, ATKINS H, et al: Radiopharmaceuticals XXVII. ^{18}F-labeled 2-deoxy-2-fluoro-D-glucose as a radiopharmaceutical for measuring regional myocardial glucose metabolism in vivo: Tissue distribution and imaging studies in animals. *J Nucl Med* 18: 990–996, 1977

15. PHELPS ME, HOFFMAN EJ, HUANG SC, et al: ECAT: A new computerized tomographic imaging system for positron-emitting radiopharmaceuticals. *J Nucl Med* 19: 635–647, 1978

16. PHELPS ME, HOFFMAN EJ, MULLANI NA, et al: Application of annihilation coincidence detection to transaxial reconstruction tomography. *J Nucl Med* 16: 210–224, 1975

17. SOKOLOFF L, REIVICH M, KENNEDY C, et al: The [^{14}C] deoxyglucose method for the measurement of local cerebral glucose utilization: Theory, procedure and normal values in the conscious and anesthetized rat. *J Neurochem* 28: 897–916, 1977

18. PHELPS ME, HOFFMAN EJ, HUANG SC, et al: Positron Tomography: An in vivo autoradiographic approach to measurement of cerebral hemodynamics and metabolism. In *Cerebral Function, Metabolism and Circulation*, Ingvar DH, Lassen NA, eds. Copenhagen, Munksgaard, 1977, pp 446–447

19. ROSE CP, GORESKY CA: Vasomotor control of capillary transit time heterogeneity in the canine coronary circulation. *Circ Res* 39: 541–554, 1976

20. OLSON RE: Physiology of cardiac muscle. In *Handbook of Physiology: Circulation*, Hamilton WF, Philips D, eds, vol. 1, Baltimore, Williams and Wilkins Co., 1962, pp 199–237

21. REIVICH M, KUHL DE, WOLF A, et al: Measurement of local cerebral glucose metabolism in man with ^{18}F-2-fluoro-2-deoxy-G-glucose. In *Cerebral Function, Metabolism and Circulation*, Ingvar DH, Lassen NA, eds. Copenhagen, Munksgaard, 1977, pp 190–191

22. SOLS A, CRANE RK: Substrate specificity of brain hexokinase. *J Biol Chem* 210: 581–595, 1954

23. GUYTON AC: *Medical Physiology*, 5th ed. Philadelphia, W. B. Saunders Co., 1976, pp 1036–1051

EDUCATION AND RESEARCH FOUNDATION GRANTS

The Education and Research Foundation of the Society of Nuclear Medicine welcomes applications for two of its projects.

Medical Student Fellowship Program: This educational project is designed to stimulate interest among medical students in the United States and Canada in the field of nuclear medicine. It will make it possible for interested and qualified students to spend elective quarters and summers in active nuclear medicine laboratories working and associating with experts in the field. Maximum grant: $1,000. Application letters in duplicate, including a description of the project and budget, should be sent to the President of the Foundation, c/o Society of Nuclear Medicine, 475 Park Avenue South, New York, New York 10016.

Mallinckrodt Fellowship: A $1,000 grant is awarded for graduate research in basic medical science related to the physical or biochemical aspects of nuclear medicine.

Pilot Research Grants in Nuclear Medicine: The goal of this research support is to provide limited sums of money to scientists to support deserving projects that are pilot in nature. It is hoped that it will make is possible for nuclear medicine scientists to apply for small sums of money for clinical and basic research, and to get a decision within a short-time following application. The grants will not support salaries, major equipment purchases or travel, but are designed to provide essential materials so that innovative ideas can be quickly tested. Maximum grant $1,000. Application forms are available from the President of the Foundation, c/o Society of Nuclear Medicine, 475 Park Avenue South, New York, New York 10016.